Fabrication of Mo microcones for volcano-structured double-gate Spindt-type emitter cathodes using triode high power pulsed magnetron sputtering

Running title: Fabrication of Spindt emitter cathode by HPPMS

Running Authors: Nakano et al.

Takeo Nakano [a)], Tomoki Narita, Kei Oya

Seikei University, Department of Materials and Life Science, 3-3-1 Kichijoji-Kita, Musashino, Tokyo 180-8633, Japan

Masayoshi Nagao, Hisashi Ohsaki

National Institute of Advanced Industrial Science and Technology (AIST), 1-1-1 Umezono, Tsukuba, Ibaraki 305-8568, Japan

[a)] Electronic mail: nakano@st.seikei.ac.jp

In this study, an array of Mo cones for volcano-structured Spindt-type micro electron emitters were fabricated. A recently-developed triode high power pulsed magnetron sputtering system was used to control the positive plasma potential and efficiently accelerate ion species. By applying a proper positive voltage to the additional electrode, we obtained good cone shapes with high aspect ratios in a water-cooled microcavity structure made of two resist layers, which was previously impossible by conventional vacuum evaporation techniques. The effects of ion acceleration on the alignment of ions along the normal direction, as well as on the stress in the deposited film, are discussed. The former is important for the formation of sharp cones, while the latter is crucial for achieving stable fabrication.

I. INTRODUCTION

A Spindt-type emitter is a kind of microfabricated vacuum electron emitter originally developed by Spindt at the Stanford Research Institute.[1] Each emitter consists of a conical-structured cathode with a sharp tip to concentrate the electric field for efficient emission of electrons. Spindt-type emitters have good electron emitter characteristics (high current density, emission uniformity, and reliability), and are expected to be applied in various devices, for example in the form of a field emitter array (FEA) in field emission displays.[2]

Conical cathodes for Spindt-type emitters have been fabricated via vacuum evaporation of emitter material into a microcavity structure with holes of ~0.5 μm diameter in its ceiling. Since the holes close gradually as the deposition proceeds, the emitter material forms conical structures by the end of the deposition process. In original Spindt-type emitters, the cavity structure is made of an insulating oxide layer sandwiched between metal layers. The bottom metal layer forms a cathode pattern, while the top metal layer, which contains the holes, functions as gate electrode. The top surface of the cavity structure is further covered with an additional material used as a sacrificial layer in the lift-off process applied after the emitter material deposition.

Recently, one of the authors proposed another configuration of this emitter, named a “volcano-structured” Spindt-type emitter.[3] In this process, the microcavity structure is prepared by two resist layers: the top layer an ordinary photoresist, and the bottom layer a non-photosensitive “lift-off” resist soluble in the same solvent as the top layer. After the gate hole pattern is exposed, the substrate is dipped into the solvent for a

controlled period of time. Through this process, the bottom layer is isotropically etched and the cavity structure formed. Subsequently, the emitter material is deposited to form conical emitter structures inside the cavities. After deposition, the resist layers are removed together with the overcoated emitter material by lift-off. Therefore, only the conical emitters are left on the substrate. The above fabrication process is summarized in Fig. 1.

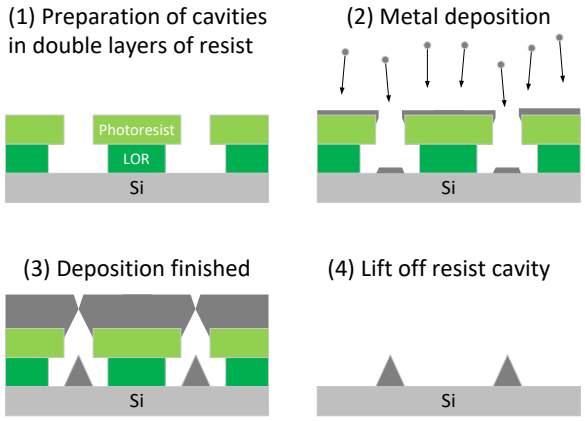

FIG. 1. (Color online) Preparation process of Mo cones for volcano-structured Spindt-type emitters. LOR in (1) denotes “lift-off” resist.

After preparing the emitters, the gate electrode is prepared using the etch-back process[4] to form volcano-structured emitters. The double-gated volcano structure, which consists of two electrodes for the extraction and focusing of electrons, can be prepared by repeating the etch-back process. This structure has been proven to show excellent electron emission characteristics,[5,6] and is expected to be a crucial part of ultrahigh sensitivity television cameras.[7]

Historically, the emitter cathode material has been deposited using vacuum evaporation. For the effective and stable operation of the emitter at high emission current densities, a refractory metal is the material of choice. However, refractory metals are notorious for their very high tensile stress when deposited at low substrate temperatures[8]. Therefore, to avoid delamination of the deposited material, the substrate has to be heated to lower the tensile stress[9]. Since resist cavities cannot withstand such high substrate temperatures, as a compromise Ti[3,10] and Ni[6] emitters have been used as the cathode material for volcano-structured double-gate Spindt-type emitters instead. There is another drawback of vacuum evaporation. It is relating to the requirement for the gradual closure of cavity holes to achieve sharp tip structures. To achieve this, the deposition flux has to be highly aligned along the normal of the substrate, requiring a long source-to-substrate distance. As a result, the preparation system tends to be bulky, and large area FEAs are hard to prepare.

To simultaneously overcome the above problems, we propose the use of ionized vapor deposition.[11,12] The ionized atoms can easily be accelerated by introducing a potential drop between the plasma bulk and the substrate. By increasing the atomic energy, various aspects of deposited films can be modified, including structure, density, number of defects, and stress.[13–15] For example, it is particularly well-known that increasing the incident energy (or incident momentum) of depositing atoms results in the transition of tensile to compressive stress.[16,17] We can therefore expect that high tensile stress in refractory metal films can be lowered by using this technique even on low temperature substrates.

In addition, the incident direction of depositing species can be aligned with the substrate normal by acceleration of ions in the sheath region in front of the substrate. In fact, achieving this directivity was the original motivation for ionized physical vapor deposition (IPVD) in order to improve the sidewall and bottom coverage in trenches and vias with high aspect ratios.[11,18] The alignment of incident ions enables a shorter distance between the source (target) and the substrate, as well as the production of larger-sized FEAs.

We have previously attempted to fabricate Spindt-type emitter cathodes by using a high power pulsed magnetron sputtering (HPPMS) technique. HPPMS is a variant of IPVD that produces a high density plasma with short pulse powers to ionize sputtered atoms efficiently.[19–21] The potential drop between the plasma bulk and the substrate is generally realized by applying a negative bias to the substrate. If a positive plasma potential can be controlled, on the other hand, a potential difference can be formed between the plasma and a grounded substrate, which improves the design flexibility of the sputter deposition system. We previously proposed two techniques to achieve the above.

One method is to introduce a positive target bias voltage during the pulse-off period of HPPMS. It was shown that the plasma potential of the afterglow period was raised, and the structure of the deposited films on a water-cooled room temperature substrate could be modified.[22] This technique was applied to Spindt-type emitter fabrication, and Mo emitter structures of varying height could be prepared inside the cavities.[3,9] It should be noted that DC operation using the same sputtering deposition

system resulted in very low structures due to the random incidence of sputtered atoms and fast occlusion of the cavity holes.

Another method we developed more recently is the triode HPPMS system that consists of a chimney-like electrode on top of the sputter gun for control of the plasma potential through the applied voltage. It was demonstrated that the plasma potential was raised in accordance with the cap voltage during not only the afterglow period, but also the pulse-on period. This potential difference between the plasma bulk and the substrate throughout the discharge enabled effective use of ionized atoms. As a result, the film structure could be modified using a significantly lower plasma potential (20-40 V) compared with the pulse-off target bias method (~100 V).[23]

In the current study, we used triode HPPMS for the preparation of volcano-structured Spindt-type emitters using Mo. Several preparation conditions for Mo metal deposition on the double-layered resist cavities were varied, such as the target to substrate distance, cap voltage, and discharge gas pressure. Obtained emitter structures were observed using a secondary electron microscope (SEM). Under specific conditions, sharp emitter structures could be obtained, preferable for Spindt-type emitters.

II. EXPERIMENTAL

Microcavities with holes were fabricated on a silicon wafer using the double layers of resists. The top photoresist layer was exposed to a hole pattern with 0.5 μm diameter, and etched together with the bottom lift-off resist layer to form the cavities. Details of the fabrication process are given in our previous report.[10]

Mo was deposited on top of the cavities using triode HPPMS. In a previous triode system,[23] we added a chimney-like electrode on top of the conventional sputter gun. In this system, however, the anode cap of the magnetron sputter gun, which covers the target peripherally at a distance of ca. 0.5 mm from the target, was insulated from the grounded chamber, and positive voltages V_c could be applied to it directly (Fig. 2). The sputter gun was equipped with a Mo target of 2 inch in diameter and was located along the symmetric axis of the sputter chamber, which was a cylinder with an inner diameter and height of 20.1 cm each. The chamber was routinely pumped down to 5×10^{-5} Pa prior to the deposition.

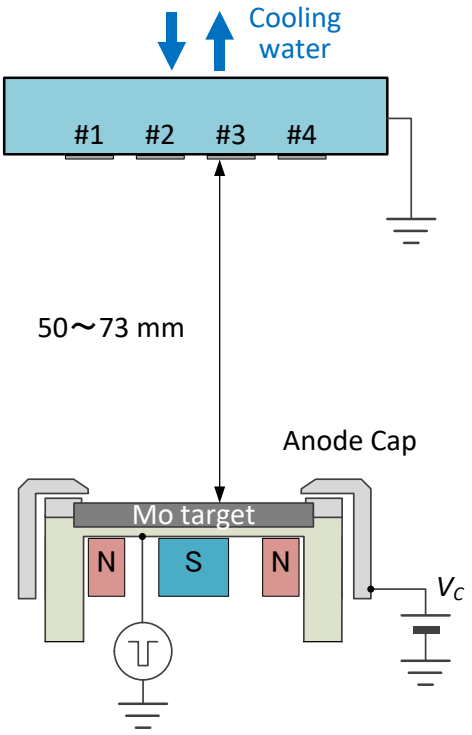

FIG. 2. (Color online) Schematic of Triode high power pulsed magnetron sputtering (HPPMS) configuration. N and S in the figure denote the poles forming the magnetron.

The plasma discharge conditions were as follows: Ar gas pressures of 0.6-3.0 Pa, pulse frequency of 200 Hz, and duty ratio of 5%. The cap voltage V_c was varied between 20-60 V. The time-averaged total electrical power supplied to the discharge volume (by both the pulse power source connected to the target and the DC power supply connected to the cap electrode) was set at 100 W using the same procedure as in our previous report[23]. The plasma potential increase in accordance with V_c was checked using the Langmuir Probe (Scientific Systems, SmartProbe) before deposition experiments.

Si wafer with cavity structures were cut into substrate pieces 1 cm width and 2.54 cm length, and tightly bound to the substrate holder as shown in Fig. 2. The holder was made of Cu and was cooled by circulating water. In most of the deposition runs, the cavity substrate was set at #2 position in Fig. 2, while a stock Si wafer substrate of the same dimension was set at #3, mainly used to determine the deposited film thickness. The holder was located 50 or 73 mm above the target surface. The typical deposition duration was 90 minutes. After deposition, the resist layers were removed by dipping the sample into an organic solvent (*N*-methyl-2-pyrrolidone; NMP) to obtain Mo conical structures. Before and after the lift-off process, samples were cleaved and their cross-sections were observed using an SEM (JEOL, JSM-6510).

III. RESULTS AND DISCUSSION

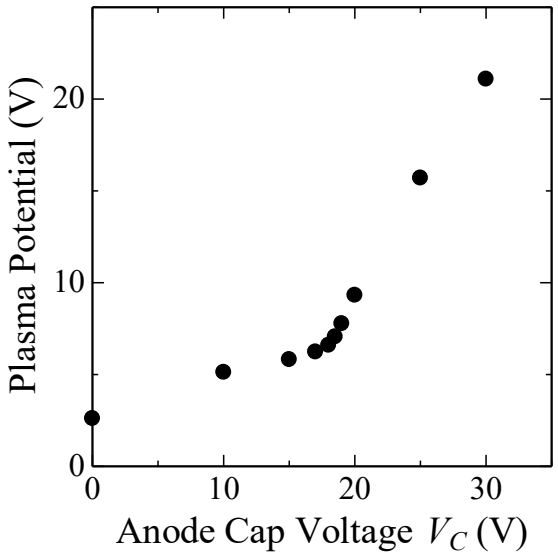

FIG. 3. Plasma potential vs. Anode cap voltage measured using the Langmuir probe. Gas pressure was 1 Pa, and the potential was recorded 200 μs after ignition of the pulse discharge using a 200 Hz frequency and 5% duty cycle.

Before depositions, plasma parameters were evaluated using time-resolved Langmuir probe measurements. Instead of the substrate holder, the probe was inserted in the chamber along the symmetric axis. The probe consisted of a tungsten wire of 0.38 mm diameter and 10 mm length, the remainder of which was shielded by an alumina tube. The probe apex was located at 50 mm from the target surface. The measurement details were the same as those described in our previous study.[23] Figure 3 shows the obtained plasma potential as a function of the V_c at an Ar gas pressure of 1 Pa. The data shown in Fig. 3 were recorded at 200 μs after plasma ignition (note that the high power pulse duration was 250 μs). The plasma potential increased in accordance with V_c. At lower cap voltages (V_c < 18 V), the increase of the potential was rather subtle, while it

increased almost linearly at unity slope when the cap voltage exceeded 20 V. A similar trend was reported with the prototype of the triode system equipped with the chimney-like electrode[23]. The electron density during the pulse-on period was 2-3×10^{17} m^{-3}.

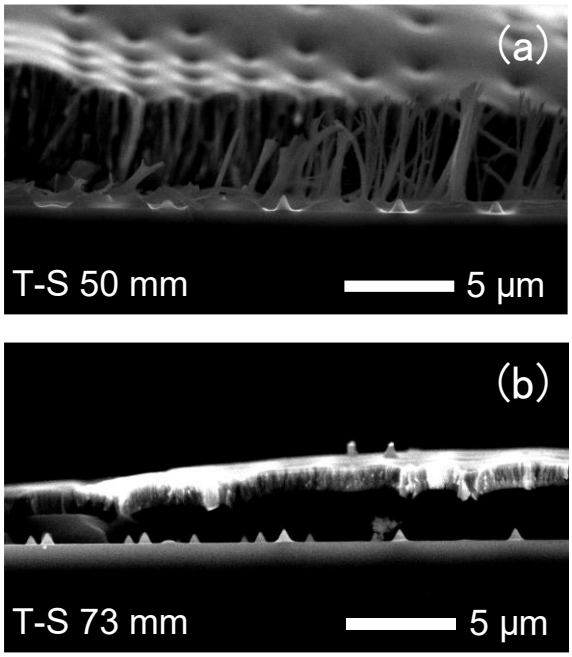

FIG. 4. Cross-sectional scanning electron microscope (SEM) images of Mo-deposited samples on double resist cavity substrates at a (a) target to substrate (T-S) distance of 50 mm and a (b) T-S distance of 73 mm. The gas pressure was 1 Pa and the anode cap voltage was 40 V.

Initially, we fixed the Ar gas pressure and pulse discharge conditions, and studied the effects of the target to substrate (T-S) distance on the deposited emitter cathode structure. Figure 4 shows the cross-sectional SEM images of deposited samples at different T-S distances, both deposited using a cap voltage of 40 V. These images were observed for the samples cleaved before the lift-off process. The resist cavities in the case of a 50 mm T-S, resist cavities were seriously deformed, as if they had melted during the

deposition process (Fig. 4(a)). In this case, the shapes and heights of Mo cones were found to be highly variable, which suggests random closure of cavity holes by thermal load-induced transformation. This might be partly due to the slightly unbalanced magnetron configuration of the sputter gun, by which we expected the spread of plasma near the substrate surface, enhancing the directivity and energetic incidence of deposition species.

By increasing the T-S distance, the deformation of the resist cavity was greatly alleviated, as shown in Fig. 4(b). A certain deformation still remained, but this deformation seemed to occur at the cleavage stage, possibly due to stress in the overcoated Mo layer. It was also found that the uniformity of the Mo cone structures was very much improved. Therefore, we continued Mo deposition experiments mainly at a T-S distance of 73 mm.

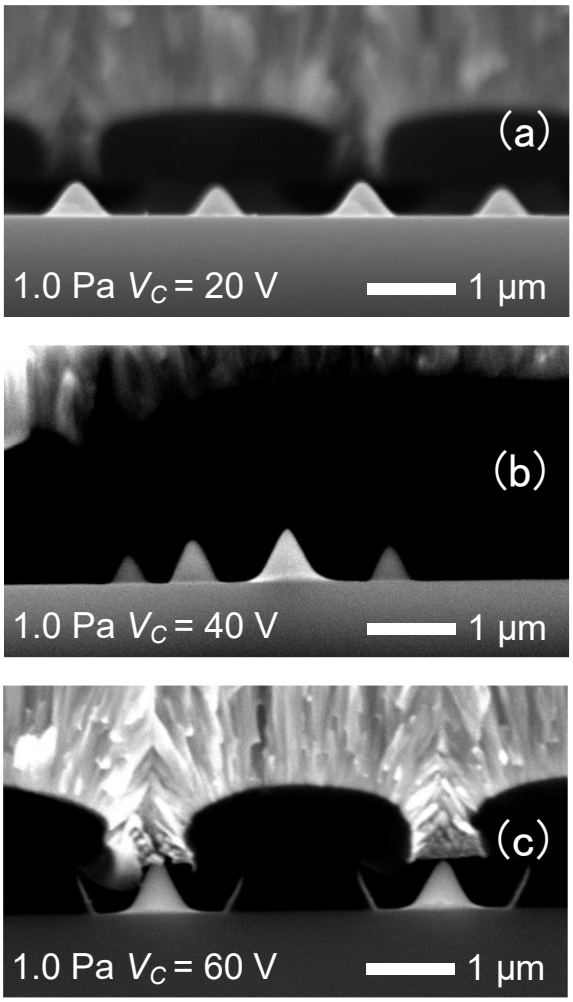

FIG. 5. Dependence of the Mo cone shape on the anode cap voltage.

The dependence of the Mo cone shape on the anode cap voltage was studied by fixing the gas pressure at 1 Pa and the T-S distance at 73 mm. Figure 5 shows selected SEM images of the cross-section of samples before the lift-off process. The structure of the cones was also observed by SEM after the lift-off process, and the aspect ratios of the cones were measured using the SEM images. Aspect ratios were determined by dividing the half height of the cone by the full width at the half maximum (FWHM), because the relative uncertainty in FWHM measurements was less than that using the base cone diameters. Aspect ratios of 5-6 cones were measured in each sample, and the average and

standard deviation are plotted in Fig. 6. The results for samples deposited at a T-S of 50 mm and V_c of 40 V are also plotted, which shows a lower average height and poor shape uniformity in comparison with cones prepared at a T-S of 73 mm.

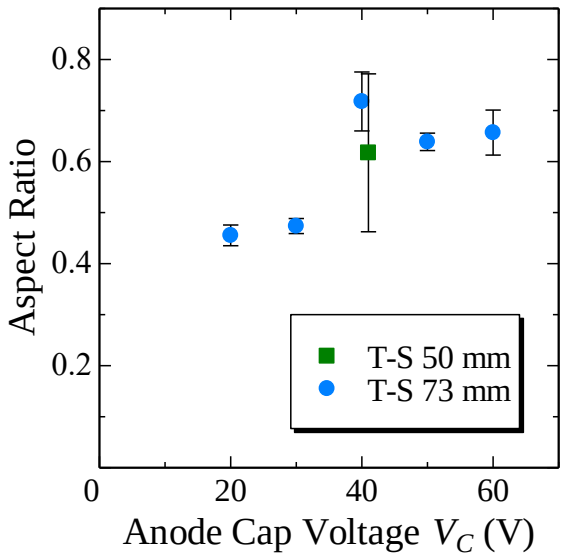

FIG. 6. (Color online) Dependence of the aspect ratio of Mo cones on the anode cap voltage. The gas pressure was fixed to 1 Pa.

Before entering into the detailed discussion of the effect of V_c , the growth mechanism of the emitter cones we are expecting under the triode HPPMS is described. By increasing V_c , the larger plasma potential is achieved as demonstrated in Fig. 1. The potential difference between the plasma bulk and the substrate is applied to the plasma sheath formed in front of the substrate. In the HPPMS plasma, considerable part of the sputtered Mo atoms are expected to be ionized, and accelerated by this sheath voltage. This lead to the energetic impingement of these ions along the electric field lines, which is formed perpendicular to the substrate surface. Therefore, the normal incidence of Mo atoms, which is favorable for the sharp cone formation, is realized. Slanted incidence of

the atoms, which is unavoidably included in the Mo flux, result in the deposition of such atoms on the sidewall of the cavity hole, hence the hole is gradually tightened. If this occurs too fast, only a low mound rather than a cone is obtained inside the cavity, which was actually demonstrated in case of the DC sputtering[3]. On the other hand, if the fraction of the sidewall deposition can be controlled properly, desirable shape of the cone should be available. In fact, in the pioneering work by Spindt utilizing the vacuum evaporation[1], two evaporation sources with different incidence angles were equipped and their evaporation rates were independently regulated to control the closure rate.

The sharpest conical structures (i.e., with highest average aspect ratio) could be obtained at V_c = 40 V. Lower and higher V_c values resulted in a decrease in aspect ratio. Considering the directivity of the ionized atoms, higher plasma potentials are preferable. At an argon gas pressure of 1 Pa, many sputtered Mo atoms reach the substrate before thermalization[24,25], and are therefore expected to retain their initial energy, which is in the range of 1-10 eV[26]. Since the speed of atoms is proportional to the square root of the energy, differences in potential drop across the sheath, expected to be 10-50 V in these experiments, may have a significant effect on the degree of alignment of ionized metal atoms. An increase in incident atom energy is also expected to contribute to the lowering of tensile stress, which was the original reason why vacuum evaporation could not be applied to Mo deposition on resist cavities. However, when the energy is too high, this film stress generally turns compressive,[16] which can also result in destruction of the cavity structure and/or unexpected closure of holes due to deformation of the resist layer. Since the bending torque applied to the resist layer may increase with an increase in film thickness in cases where the film experiences biaxial compressive stress,[27] holes may

unexpectedly close by the torque during deposition. This should result in inferior aspect ratios and duller apices of the cones. This change in stress polarity, from tensile to compressive, has been known to occur when the energy per arrival atom is a few tens of electron volts,[13,28,29] which is within range in this study. Therefore, too high anode cap voltages and the resultant particle energies may deteriorate the sharpness of the prepared emitter cones.

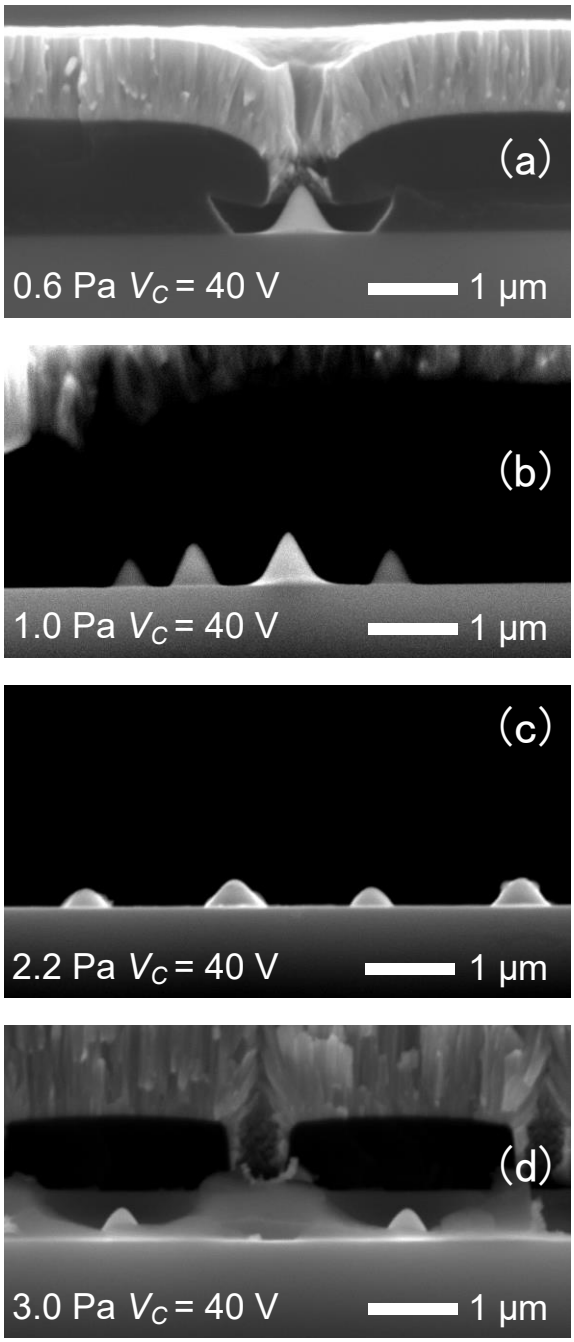

FIG. 7: Dependence of Mo cone shapes on Ar gas pressure.

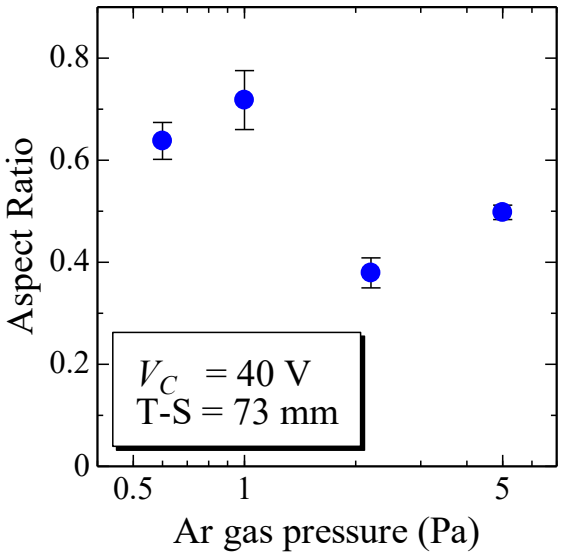

FIG. 8. (Color online) Dependence of the aspect ratios of Mo cones on the discharge gas pressure.

The dependence of the cone shape on gas pressure is shown in Figs. 7 (SEM images) and 8 (aspect ratios). In series of experiments, the anode cap voltage was set at 40 V, and the T-S distance at 73 mm. The observation and measurement procedures were identical as those used in Figs. 5 and 6. From Fig. 7, it can be seen that higher gas pressures resulted in cones with low mound structures with gentle slopes. On the other hand, samples prepared at pressures at or below 1 Pa were found to have sharper cones. The latter is also confirmed by the dependence of apex ratio on gas pressure in Fig. 8.

The decrease in sharpness of the cones at higher gas pressures can be ascribed to two reasons. First, an increase in random incidence angles of Mo ions occur at the substrate sheath edge, due to the collision and scattering of sputtered Mo atoms by ambient Ar gas. In our previous calculations,[24] the product of pressure and distance of Mo for thermalization was about 14 Pa·cm. This means that at 2 Pa, a significant part of

Mo atoms/ions lose their initial direction from the target to the substrate after traveling 7 cm. When ions arrive at the sheath edge with oblique incidence with the energy of a few eVs, they cannot be completely aligned to the substrate's normal by the potential drop of the sheath region. In the worst case, for an initial energy of 1 eV and potential drop of 30 V, the maximum final angle can be calculated as: $\tan^{-1}(1/\sqrt{30}) \approx 10.3°$. This effect leads to deposition of atoms on the sidewalls of cavity holes and thus their fast closure.

Secondly, higher gas pressures result in collisional scattering of Mo ions inside the sheath. When the ions collide with neutral species and exchange charge and/or momentum during acceleration in the sheath, they do not fully aligned along the substrate's normal. In the case of Ar ion to Ar neutral, momentum transfer and charge exchange collision cross sections are on the order of 10^{-18} m^2 and $4\text{-}5\times10^{-19}$ m^2, respectively.[30] This means that at 1 Pa and 300 K, the mean free path is on the order of 4-10 mm. On the other hand, it was reported[31] that the electron-free sheath thickness with potential drop of 30 V was a few centimeters for plasma whose electron temperature T_e was 2.4 eV and electron density n_e was 2.0×10^{13} m^{-3}. This thickness scales with the Debye length, which is proportional to $\sqrt{T_e/n_e}$. When $n_e \approx 10^{17}$ m^{-3}, the sheath thickness is about 0.2 mm. Considering that the collision mean free path is inversely proportional to the gas pressure, collisions inside the sheath cannot be neglected and should have some effect on the directivity of the incident ion flux. We suggest that lower gas pressures should lead to better structures, provided that a stable pulse discharge can be maintained.

We should note again that these results were obtained at the substrate position #2 in Fig. 2 as described in the experimental section. In the preliminary stage of this research, we also placed the cavity substrate at position #1 and compared the obtained

cone shapes. It was found that slightly low and slanted cone shapes were obtained at #1, which may be due to the difference in the ratio of neutral and ionized atoms and their fluxes. Further research is necessary for the uniformity of the cone shapes utilizing the target of large size, which is included in our research plan in the near future along with the fabrication and demonstration of working emitters.

IV. SUMMARY

We have here demonstrated that Mo cones could be obtained inside resist cavities at room temperature using a triode high power pulsed magnetron sputtering (HPPMS) system. A positive plasma potential was confirmed, which should lead to normal incidence and higher incident energy of depositing Mo ions. The aligned incidence was expected to contribute to the formation of high aspect ratio cones, and the higher energy to help the suppression of tensile film stress at room temperature. In this study, optimal structures were obtained at an anode cap voltage V_c of 40 V at a gas pressure of 1 Pa and target to substrate distance of 73 mm. Higher or lower anode cap voltages, as well as higher gas pressures, resulted in lower aspect ratios of the formed cones. In particular, it was found that a plasma potential that was too high resulted in strong compressive stress in the deposited films, which broke or deformed the resist cavities.

In general, the formation of Mo cone structures was much improved by triode HPPMS deposition compared with conventional vacuum evaporation and previous pulse-off voltage-modulated HPPMS deposition. The experimental results here indicate that parameter optimization improves apex sharpness (*i.e.,* small curvature radius) and process stability. This optimization can be achieved by precise control of the film stress

using HPPMS, which may result in valuable information for many additional applications using HPPMS.

ACKNOWLEDGMENTS

We wish to thank Mr. Shunichi Yoshizawa at the National Institute of Advanced Industrial Science and Technology (AIST) for his assistance in fabricating the photoresist microcavity structures. We also wish to thank Kengo Nishitani at Seikei University for his assistance with the experiments.

[1] C.A. Spindt, J. Appl. Phys. **39**, 3504 (1968).

[2] C.A. Spindt, I. Brodie, C.E. Holland, and P.R. Schwoebel, in *Vacuum Microelectronics*, edited by W. Zhu (Wiley, Spindt2004, 2004).

[3] M. Nagao, T. Yoshida, T. Nishi, and N. Koda, in *Tech Dig. IVNC 2012* (IEEE, 2012), pp. 110–111.

[4] M. Nagao, T. Yoshida, S. Kanemaru, Y. Neo, and H. Mimura, Jpn. J. Appl. Phys. **48**, 06FK02 (2009).

[5] Y. Honda, M. Nanba, K. Miyakawa, M. Kubota, M. Nagao, Y. Neo, H. Mimura, and N. Egami, IEEE Trans. Electron Devices **63**, 2182 (2016).

[6] M. Nagao, Y. Gotoh, Y. Neo, and H. Mimura, J. Vac. Sci. Technol. B **34**, 02G108 (2016).

[7] Y. Honda, M. Nanba, K. Miyakawa, M. Kubota, M. Nagao, Y. Neo, H. Mimura, and N. Egami, J. Vac. Sci. Technol. B **34**, 52201 (2016).

[8] J.A. Thornton and D.W. Hoffman, Thin Solid Films **171**, 5 (1989).

[9] M. Nagao and T. Yoshida, Microelectron. Eng. **132**, 14 (2015).

[10] M. Nagao and S. Yoshizawa, in *Tech. Dig. IVNC 2014* (IEEE, 2014), pp. 226–227.

[11] J.A. Hopwood, *Ionized Physical Vapor Deposition* (Academic Press, San Diego, 1999).

[12] U. Helmersson, M. Lattemann, A.P. Ehiasarian, J. Bohlmark, and J.T. Gudmundsson, Thin Solid Films **513**, 1 (2006).

[13] S.M. Rossnagel and J.J. Cuomo, Thin Solid Films **171**, 143 (1989).

[14] D.M. Mattox, J. Vac. Sci. Technol. A **7**, 1105 (1989).

[15] I. Petrov, P.B. Barna, L. Hultman, and J.E. Greene, J. Vac. Sci. Technol. A **21**, S117 (2003).

[16] H. Windischmann, J. Vac. Sci. Technol. A **9**, 2431 (1991).

[17] H. Windischmann, Crit. Rev. Solid State Mater. Sci. **17**, 547 (1992).

[18] S.M. Rossnagel, J. Vac. Sci. Technol. B **16**, 2585 (1998).

[19] J.T. Gudmundsson, N. Brenning, D. Lundin, and U. Helmersson, J. Vac. Sci. Technol. A **30**, 30801 (2012).

[20] K. Sarakinos, J. Alami, and S. Konstantinidis, Surf. Coat. Technol. **204**, 1661 (2010).

[21] N. Britun, T. Minea, S. Konstantinidis, and R. Snyders, J. Phys. D. Appl. Phys. **47**, 224001 (2014).

[22] T. Nakano, N. Hirukawa, S. Saeki, and S. Baba, Vacuum **87**, 109 (2013).

[23] T. Nakano, T. Umahashi, and S. Baba, Jpn. J. Appl. Phys. **53**, 28001 (2014).

[24] T. Nakano and S. Baba, Jpn. J. Appl. Phys. **53**, 38002 (2014).

[25] T. Nakano, R. Yamazaki, and S. Baba, J. Vac. Soc. Jpn. **57**, 152 (2014).

[26] R. Behrisch and W. Eckstein, editors , *Sputtering by Particle Bombardment: Experiments and Computer Calculations from Threshold to MeV Energies* (Springer, Berlin, 2007).

[27] M. Ohring, *Materials Science of Thin Films* (Academic Press, San Diego, CA, 2002).

[28] T.C. Huang, G. Lim, F. Parmigiani, and E. Kay, J. Vac. Sci. Technol. A **3**, 2161 (1985).

[29] J.J. Cuomo, J. Vac. Sci. Technol. **20**, 349 (1982).

[30] A. V. Phelps, J. Phys. Chem. Ref. Data **20**, 557 (1991).

[31] L. Oksuz and N. Hershkowitz, Phys. Rev. Lett. **89**, 145001 (2002).

Figure Captions

FIG. 1. (Color online) Preparation process of Mo cones for volcano-structured Spindt-type emitters. LOR in (1) denotes “lift-off” resist.

FIG. 2. (Color online) Schematic of Triode high power pulsed magnetron sputtering (HPPMS) configuration. N and S in the figure denote the poles forming the magnetron.

FIG. 3. Plasma potential vs. Anode cap voltage measured using the Langmuir probe. Gas pressure was 1 Pa, and the potential was recorded 200 μs after ignition of the pulse discharge using a 200 Hz frequency and 5% duty cycle.

FIG. 4. Cross-sectional scanning electron microscope (SEM) images of Mo-deposited samples on double resist cavity substrates at a (a) target to substrate (T-S) distance of 50 mm and a (b) T-S distance of 73 mm. The gas pressure was 1 Pa and the anode cap voltage was 40 V.

FIG. 5. Dependence of the Mo cone shape on the anode cap voltage.

FIG. 6. (Color online) Dependence of the aspect ratio of Mo cones on the anode cap voltage. The gas pressure was fixed to 1 Pa.

FIG. 7: Dependence of Mo cone shapes on Ar gas pressure.

FIG. 8. (Color online) Dependence of the aspect ratios of Mo cones on the discharge gas pressure.